RECENT WORK ON THE HELIX STRUCTURE AND PROPERTIES OF TANDEM HELIX COMBINATIONS FOR THE ACCELERATION OF HEAVY IONS

H. Klein, P. Junior, A. Schempp
Inst. f. Angew. Physik, Univ. Frankfurt
P. Finke, H. Herminghaus[+)], J. Klabunde, L. Lehr
GSI-Darmstadt, Außenstelle Univ. Frankfurt
[+)] On leave of absence from Inst. f. Kernphysik, Univ. Mainz

Abstract

Field stabilization in helical resonators can be achieved by compensating the structure in a relative simple manner. The influence of termination effects on field distribution and resonant frequencies of λ/2-helices is investigated. A modified normal conducting Talix accelerator in pulsed operation is described. Some figures are given for the expected beam performance of postaccelerators with superconducting helices.

Introduction

In 1971 we proposed a Helix Tandem combination for acceleration of heavy ions in CW operation [Talix] (1),(2). In the last months the work was concentrated on a pulsed version of Talix (3), mainly in order to reduce the operating costs. Other work - partly in close cooperation with the linac group of the Kernforschungszentrum Karlsruhe - was directed to the RF properties of the helix structure. So calculations and measurements of axial and surface fields were done, which are of special interest for superconducting helices (4). Here the properties of λ/2-helices are briefly discussed and a method for compensation of the helix structure is described.

Field Stabilization

In 1971 vibrational instabilities were observed when testing a 1 m long, dielectrically stemmed, normal conducting π-mode helix section in CW operation at high power. Obviously, a positive feedback involving electromechanical forces between the windings of the helix led to excitation of longitudinal vibrations of about 100 Hz. This instability, however, was apparently not identical with the one described by Karliner, Schulze et al. (5),(6); its threshold was much lower and it occured on both sides of the resonance curve. It was believed that this might be due to collective vibrations of the 7 λ/2-cells of the section, whereas the papers cited refer to single cavities only. Meanwhile some experimental work is done on this and it seems that the difficulties can be overcome by field stabilization, though the feedback mechanism is not yet totally revealed. There is, however, some evidence that the effect of unflatness is involved, because the section could be operated without vibrations after it had been compensated. But it should be stated, that at the same time the RF system and the amplitude control had been improved. The method of compensation used is described below. Another approach is to attach hollow, mercury-filled balls to the helix, by which is obtained simultaneously lowering the mechanical Q of the helix and compensation. A wave guide of this kind, working in a π/3-mode, is now in preparation.

Some attempts have been made to investigate the influence of several types of inhomogenities on the helix wave guide, such as stems, wave guide ends etc. The investigation by aid of the sheath model leads to rather cumbersome calculations and did not give practical results yet. This work will be continued, however. Other investigations were done on the basis of the transmission line theory that has been developed several years ago especially for application to the closely wound helix (7). It has the advantage to allow the treatment of several types of inhomogenities in a very simple and straightforward way. On the other hand, its results are not very precise when applied to our Talix type helices, which are not wound closely. They are, however, precise enough to describe the effects qualitatively in the right manner and to give numerical values of the right order of magnitude. Without going into the details it should just be mentioned that this theory uses the magnetic flux as one of the conjugate variables and that it gives a pair of cutoff modes as solutions besides the usual forward and backward traveling waves. In general, these cutoff modes are needed to fulfill the boundary conditions at an inhomogenity.

On the basis of this model the influence of the wave guide ends on field configuration and resonance frequency was investigated (s. next paragraph).

The transmission line theory has been used further to calculate the effects of inhomogenities like stems etc. It turned out, for instance, that a metallic stem between helix and shield at high frequencies acts like a shunt capacitance of the order of 10 pF (8). This has been confirmed experimentally. Another result is that a short circuit between two neighbouring windings acts like a series capacitance of a few pF (9).

This can be used to stabilize the field distribution of dielectrically stemmed π-mode sections in a very simple way (9). It can readily be calculated, that a biperiodic structure as shown in fig. 1a will be compensated with respect to unflatness effects, if C_s and C_p fulfill the condition $\omega^2 Z^2 C_s C_p = 1$ (Z is the characteristic impedance of the unloaded line). As mentioned before, the series capacitances may be replaced in case of a helix by short circuited windings. Thus, by proper choice of the capacitances of the dielectric stems compensation can be achieved. Fortunately, the shunt capacitances needed are practically always larger than the natural capacitances of a stem; so these capacitances can be adjusted by fixing metal bodies of special shape at the stem (see fig. 2). These poncho-like bodies serve simultaneously as effective shields to protect the dielectric material of the stems from the axial electric field. The experiments show that the change in field distribution by detuning the cavity is easily reduced by a factor of 5 after compensation. Further improvements are expected by better adjusting of the capacities.

Resonance Frequencies and Fields of Half-Wavelength-Helices

While the sheath model is very well suited for long helices, differences to measurements up to 50% occur, e.g., for resonance frequencies in the case of half-wavelength-helices. Therefore calculations have been made with a combination of sheath model and transmission line theory to get the fields and resonance frequencies f or the real length L_R for a given set of parameters (10). Especially the dispersion relation of the sheath theory was introduced into the transmission line calculation. This leads to a forward and backward traveling wave and a damping mode from each end of the helix and gives in case of the resonance frequencies results within 10% accuracy.

Then with a fitparameter, which works on the slope of the damping modes, the calculations for f were tied to the experiments in one point. With this fit the resonance frequencies were calculated in the following range of parameters:

80 MHz $\leq$ f $\leq$ 120 MHz	
2.0 cm $\leq$ a $\leq$ 4.5 cm	a helix radius
s/d $\geq$ 1.5	s pitch d tube diameter

The accuracy is now better than 2%. For smaller frequencies (80 - 30 MHz) the error is still less than 5%.

This method has been used to determine the final geometric parameters of the superconducting helix sections of the Karlsruhe Proton Accelerator Project (11).

Fig. 3 shows the calculated and the measured frequencies for two examples compared to the results given by the sheath model.

Fig. 4 gives for one helix the calculated electric field E_R on the axis together with the measured field, the sine approximation for the measured field and the field of a "sheath-λ/2-helix" E_s for the same parameters. In these cases the power loss per unit length p is kept constant.

Fig. 5 shows the energy gain ΔT of particles in these four field configurations as a function of the particle energy. This is compared to the energy gain in a "sheath-λ/2-helix" with the condition that the particle velocity v_T is equal to the phase velocity v_{ph_s} calculated with the sheath model ($v_T = v_{ph_s}$, $\Delta T = \Delta T_{s_o}$). Although the amplitude of the electric field E_R is smaller, the energy gain is greater than in the corresponding sheath model field, due to the increased helix length and the fringing fields.

Fig. 6 gives the calculated maximum effective shunt impedance for standing wave operation

$$\eta_{eff} = \frac{\Delta T_R^2}{T_{s_o}^2} \cdot \frac{L_s^2}{L_R^2} = \eta_{sheath} \cdot TT^2$$

for λ/2-helices as a function of the particle energy for two examples.

TT	transit time factor
L_s	length of a λ/2-helix given by the sheath model
L_R	real length of a λ/2-helix
ΔT_R	energy gain of a particle in the field of a real λ/2-helix

Tandem Helix Accelerator for Pulsed Operation

General Remarks

In a former Talix-proposal (1),(2) a heavy ion facility was suggested, where a Tandem was followed by a Helix linac. As demanded at that time, the accelerator was dimensioned for a duty factor of 100%.

At an "informal symposium about the Heidelberg postaccelerator project", which took place on the 2nd and 3rd of June 1972, the desire of linac customers became clear, to leave the CW operation and aim toward a duty factor of 25% (12).
The argument for this change originated from the idea that ion sources deliver much higher beam currents than the Tandem machine is capable to accelerate and this is true for most ions. Therefore at pulsed operation and a duty factor of 25% the same mean beam current is obtained as at CW operation, when the beam current is increased during pulse duration by a factor of 4.

Without particle loss power consumption together with corresponding operation costs can be strongly reduced.

Studies of possibilities of a pulsed Talix started immediately after the Heidelberg symposium theoretically as well as experimentally. As it turned out that the fundamental lay-out of the linac is not altered by the pulsed design, only differences to the former CW Talix are briefly discussed here. Several alternatives are reviewed, where the aim towards higher energies for light ions is taken into consideration (3), (13).

Beam Performance of Tandem Accelerator

The terminal voltage of the MP-Tandem is scheduled to 12 MV. Tandem output energies for different ions (gas stripper in terminal) and charge states behind the second stripper (foil), corresponding to about 50% of the maximum intensity, are listed in the following table.

Ion	Tandem output energy [MeV/N]	Charge State behind 2. Stripper
^{12}C	7.0	6^+
^{16}O	4.5	8^+
^{32}S	3.0	14^+
^{40}C	2.7	17^+
^{56}Fe	1.92	20^+
^{79}Br	1.36	24^+

These charge states are higher than those assumed in (1),(2). A design where the beam is bunched and chopped between ion source and Tandem has been studied. Higher energy resolution and better time structure turn out when compared to the earlier proposal.

A further advantage of this comparatively small buncher lies in the fact that particles won't charge the Tandem, which are not accepted by the linac anyway, such that an increase of the mean beam current is made possible. Besides the second buncher at the Tandem output turns out to be shorter and more simple than the single foreseen in (1). More details are given in (12).

Radial acceptances of the linac focused by quadrupole doublets (A_{eff} = 1.5 cm mrad normalized) exceed the beam emittance as expected from the Tandem (0.056 cm mrad) by a factor of 25.

Maximum pulse length admissable and at given duty factor lowest pulse frequency are given by Tandem features, especially by the capacity of the terminal. At long pulses the terminal voltage decreases noticeably, which deteriorates energy resolution. Recent measurements indicate pulses of 1-2 msec as still tolerable. This corresponds to a duty cycle of 250-125 Hz. As the Helix possesses a rather short rise time (ca. 20 µsec), high repetition frequencies are possible without remarkable power losses during the build up time. Therefore a pulse repetition frequency of about 400 Hz at pulse durations of 0.6 msec is proposed.

Helix Postaccelerator

Determination of Accelerating Field. All versions of a pulsed Talix discussed in this report deal with compromises between RF power and accelerating electric field strengths. In the earlier Talix-proposal, CW operation gave the basis for the layout. Cooling and transmitter economy with regard to construction and operation costs suggested a mean accelerating field of E_o = 1.38 MV/m. Similar considerations concerning the pulsed machine resulted in E_o = 1.8 MV/m. This together with higher charge states (as mentioned above) gives much higher final energies. (For an example for Bromine and 14 sections (1 m long) the final energy is 7 MeV/N instead of 5.5 MeV/N.)

Synchronously the mean power is reduced by about 55%. In addition these higher electric fields are capable of accelerating Iodine to the Coulomb barrier of 5 MeV/N with only 11 sections.

Transmitters having been developed and tested in collaboration with the industry had been dimensioned for CW operation at 100 kW. With small modifications they allow pulse operation and a pulse power of about 200 kW. A power of 125 kW (during the pulse) is required in order to obtain an accelerating field of 1.8 MV/m in a section of 1 m length. Therefore there is still a reserve, which could be made use of by increase of the electric field in case of a lower charge to mass ratio of ions to be accelerated as well as for compensating unexpected additional power losses.

It is well known that the helix can be operated at very high accelerating fields (>2.2 MV/m traveling wave) without voltage break down and at low x-ray levels (some mr/h at 1 m distance).

The tendency towards electromechanical oscillations of the Helix has been suppressed successfully in CW operation by compensating the structure and by improvement of the RF system and the amplitude control. Long-time tests with pulsed operation have been performed systematically in the last time. Stable operation was possible at variation of pulse repetition frequencies within the relevant range from 200-1000 Hz, no mechanical resonances occured. They were observed, in fact, as soon as the pulse frequency approximated 100 Hz, where mechanical eigenresonances lie. At these experiments 2 MV/m couldn't be exceeded because of output power limitation of the transmit-

ter, the latter not yet having been optimized for pulse operation.
It should be stated that the helix sections in these tests had not yet been compensated. As a next step for high-power and long-time tests a compensated structure is provided. While the amplitude regulation circuit system was sufficient for the pulsed operation, the phase regulation turned out to be too slow. Nevertheless operation was stable even without phase regulation, the phase jitter didn't exceed $\pm$ 1° and a constant phase along the section was observed, which is in agreement with similar observations done at the superconducting helix at the KFZ Karlsruhe. Concerning the structure, a design based upon 1.8 MV/m still leaves enough security.

Flexibility. The section arrangement of the helix accelerator permits a rather high flexibility with respect to different ions and energies. The flexibility is limited by the length of the sections. Fig. 7 shows the transit time factor for various section lengths at 1.4 MeV/N (traveling wave approximation). The increase of the transit time factor with decreasing section length is evident. The efficiency of a $\lambda/2$-helix is illustrated in figs. 5 and 6. It is obvious that an accelerator consisting of many separate $\lambda/2$-sections has the advantage of very high flexibility. This design is under discussion for a heavy ion linac consisting of room temperature helices at Los Alamos. But the choice of the section length is a compromise between flexibility, complexity and costs. Our studies for the Heidelberg facility resulted in keeping up with the 1m sections as[+)] the costs increase considerably (factor 2-3), while the final energy is increased only for very light ions, similar to the situation with single gap cavities. Examples for three versions of superconducting helix accelerators, described later, show that flexibility exists in a wide range too if each section consists of several $\lambda/2$-cells. [+)] for shorter sections

Fig. 8 indicates the important fact that transit time factors strongly increase with phase velocity. At higher energies therefore flexibility becomes better than at the injection energy. Changes in the injection energy (reduction of Tandem terminal voltage from 12 to 10.5 MV) could be either met by a small reduction of phase velocities of the first helix sections (compared to expected normal particle velocity) or by a small (ca. 50 cm) adapting helix section (the first idea being better suited for the Bromine version, the latter for the Iodine version). This is important only if one considers the heaviest ions associated to a certain version, as the lighter ions can be accelerated at reduced terminal voltages anyhow.

There is still another kind of flexibility specific to the helix structure, i.e., either the interchange of inner conductors (with another velocity profile) or the complete interchangeability of whole sections, which leaves the optical adjustment of the quadrupoles and remaining helix sections unaltered.

If customers insist on lighter ions with higher energies at a given version, our proposition is to place corresponding sections (outer conductor, inner conductor, probes) into the design plan already. Time for such an exchange of sections is roughly estimated to be about a week, construction costs necessary do not exceed 200 kDM at 11 sections; while the Iodine versions with 11 sections delivers sulphur ions of 6 MeV/N, the interchange version delivers about 10.5 MeV/N.

Description of Different Versions. This chapter gives a short description of different versions all based upon sections 1 m long at accelerating fields of 1.8 MV/m, frequency 108.48 MHz, synchronous phase angle 30°; as a consequence the total voltage gain of a section amounts to 1.56 MV. Taking into account additional power losses (lower Q's, coupling losses) average RF power is determined to 35 kW per section at a 25% duty factor. Versions differ by numbers of sections and velocity profiles.

Fig. 9 shows the dependence of the maximum final energy on the atomic mass number for a Helix postaccelerator, laid out for Iodine. As mentioned before with only 11 sections Iodine ions are successfully accelerated above the Coulomb barrier so far. Within this profile the upper limit for Calcium reaches to 6 MeV/N. Five further sections - they could be kept in reserve for a future step - would raise this final energies to 7 MeV/N (Iodine) and 8 MeV/N (Calcium).

For a comparison, a corresponding curve is drawn for the case of 10 single resonator cavities (15). The voltage gain varies with respect to transit time factors depending on particle velocity and consequently on the mass number (for an example 1 MV/section in case of Bromine, 1.2 MV/section in case of Calcium). In accordance, final energies obtainable are relatively small (2.7 MeV/N Iodine), but increase quite fast with lower atomic mass numbers (7.3 MeV/N Calcium). This is caused by the fact that for lighter ions, the rather fast increasing Tandem output energies can be fully utilized by the single resonator cavities in contrast to a Helix linac consisting of 1 m sections.

On the other hand, it must be taken into account that helix sections are much cheaper (about a factor of 3). All parts included (RF systems, quadrupole lenses, vacuum equipment etc.) overall costs of 10 single resonators match those of 13 helix sections.

Fig. 10 gives final energies of the atomic mass number for a Bromine profile at different numbers of sections. With the installation of only 8 sections the Coulomb barrier

for Bromine is closely reached. This post-accelerator can be used up to a mass number of about 100.

To match the aim of accelerating higher ions to higher energies final energies for a Calcium velocity profile are drawn in fig. 11.

Because of the easy and cheap facility of changing sections, a Helix linac consisting of 11 sections with an Iodine and a Calcium velocity profile seems to form a promising and attractive combination.

Fig. 12 demonstrates the energy per ion as a function of the atomic mass number for several accelerator projects i.e. a 12 MV Tandem, the Berlin Cyclotron project (Vicksy), 10 single resonator cavities and some Helix linac versions. This drawing gives a picture of the differences of the accelerators. Vicksy has a constant maximum energy of 200 MeV/Ion and therefore the highest energies for light ions, but the upper mass is limited to about 40. The single resonator cavities deliver higher energies for light ions than the helix versions. Additionally, the single resonator linac is capable of accelerating all ions even heavier than Iodine, but to smaller energies of course. It should therefore be possible to extrapolate the Minilac curves toward higher masses. The Helix linac, on the other hand, is clearly superior for middleweight ions.

Beam Performance of Superconducting Helix Postaccelerators

In order to get a survey on possible beam properties, calculations were done for three versions of superconducting Helix postaccelerators.

The parameters of these hypothetic machines (frequency, maximum electric field, quadrupole lengths, drift lengths) are mainly based on data given by C.M. Jones, Oak Ridge NL (16) and W. Ramler, Argonne NL (17). Experimental and theoretical results of the work done with the superconducting helix at the Kernforschungszentrum Karlsruhe are of fundamental importance for the assumed data.

The most significant figures of these accelerators are listed below (18),(19). These linacs are optimized for Uranium and differ mainly in injection energy and velocity profile. Radial focusing is accomplished by magnetic singlets or doublets. The magnetic field gradients are moderate. In case of doublet focusing the radial acceptance exceeds the beam emittance as expected from a Tandem by a large factor.

The energy resolution at the end of the linacs is better than 1% and can be improved by a factor of ten by a debuncher behind the linac. By proper adjustment of the RF phase and amplitude a pulse width shorter than 1 nsec is expected.

The maximum energy for lighter ions is shown in figs. 13-15 for the three versions.

Input energy [MeV/N]	0.756	1.1	1.43
β [%]	4.0	4.8	5.5
Final energy for Uranium [MeV/N]	10.2	10.1	10.4
Charge state ζ of Uranium	37	36	47
Number of sections	26	30	18
Frequency [MHz]	52	120	52
Accelerating electric fieldampl.	2.0	2.3	2.0
Synchronous phase	30°	30°	30°
Helix lengths	$5 \cdot \lambda/2$	1 m	$5 \cdot \lambda/2$
Total length of Helix acc. [m] (including drift lengths)	$\sim$48	60	$\sim$34
Magnetic field gradients [kG/cm]			
a) Doublet	2-3.5	2.2-4	2.8-4.3
b) Singlet	0.8-0.9	-	0.7-0.8
Effective radial acceptances[+)] (normalized; [cm mrad])			
a) Doublet	3.2	0.9	4.2
b) Singlet	0.65	-	0.9

[+)] $\Delta\varphi_{initial} = \pm 20^{\circ}$; $(\Delta T/T)_{max} = 0.5\%$

Acknowledgements

The authors wish to thank Mrs. M. Herzfeldt for her valuable assistance in handling the data of the computer programs and for her careful drawings.

The work has been supported by Bundesministerium für Bildung und Wissenschaft and by GSI Darmstadt. The Computations were carried out at the ZRI at Frankfurt University.

References

1) H. Klein, H. Herminghaus, P. Junior, J. Klabunde
Nucl. Instr. and Meth., 97, 1, 41 (1971)

2) R. Bock, E. Grosse, H. Herminghaus, P. Junior, J. Klabunde, H. Klein
GSI Darmstadt (1971)

3) H. Klein, J. Klabunde, H. Herminghaus, P. Finke, P. Junior
Int. Rep., Frankfurt, Juli 1972

4) H. Klein, N. Merz, O. Siart
Particle Accelerators 3, 235 (1972)

5) M.M. Karliner, V.E. Shapiro, I.A. Shekktman
Sov. Phys. - Techn. Phys., 11, 1501 (1967)

6) D. Schulze
KfK-Bericht 1493, Kernforschungszentrum Karlsruhe (1971)

7) H. Herminghaus
Dissertation, Univ. Frankfurt/M. (1961)

8) H. Herminghaus
Z. Angew. Phys., Vol. 29, 3, 212 (1970)

9) H. Herminghaus
Int. Rep. 72/5, Frankfurt/M. (1972)

10) A. Schempp
Dissertation, Univ. Frankfurt (in prep.)

11) A. Citron et al.
Proc. of this conference

12) Bericht MPI H-1972-V 26
Heidelberg (1972)

13) H. Klein, H. Herminghaus, J. Klabunde
Int. Rep. 72/2, Univ. Frankfurt (1972)

14) R.H. Stokes
LASL, priv. comm. (1972)

15) D. Böhne
Unilac Arbeitsnotiz HM 106 72-1,
GSI Darmstadt (1972)

16) C.M. Jones
Oak Ridge NL, priv. comm. (1972)

17) W. Ramler
Argonne NL, priv. comm. (1972)

18) J. Klabunde, H. Deitinghoff, H. Klein, P. Junior
Int. Rep. 72/6, Univ. Frankfurt (1972)

19) J. Klabunde, H. Deitinghoff
Int. Rep. 72/7 and 72/8, Univ. Frankfurt (1972)

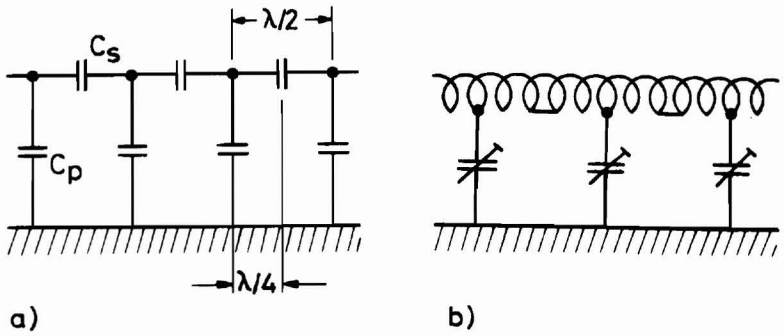

Fig. 1. a) A compensated biperiodic structure being the equivalent circuit of the compensated helix structure b).

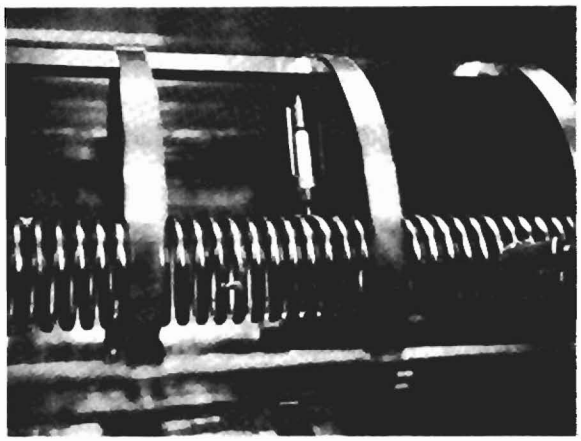

Fig. 2. Part of a compensated helix structure.

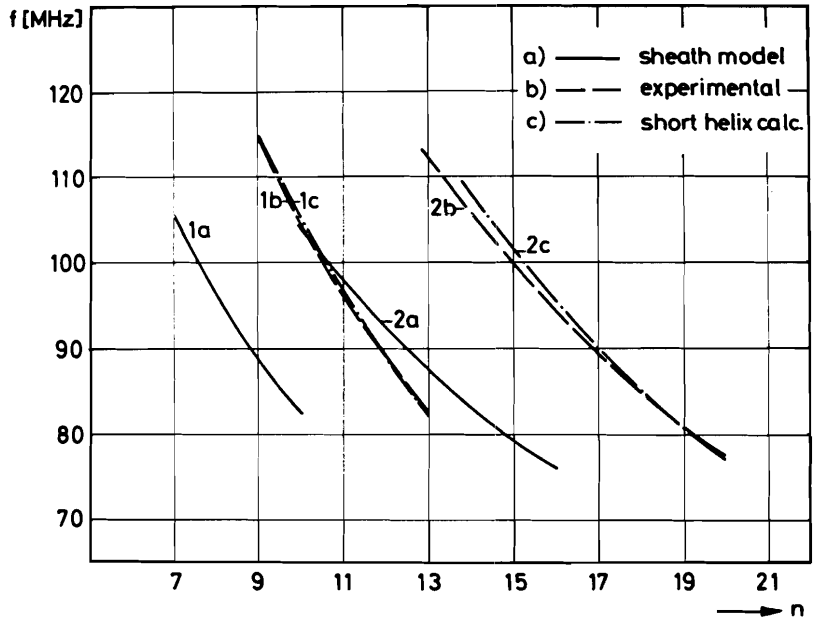

Fig. 3. Calculated and measured resonance as function of the number of windings n
1. a=3.35cm, s=1.0cm, d=0.6cm, b=12.5cm
2. a=2.45cm, s=0.6cm, d=0.4cm, b=12.5cm

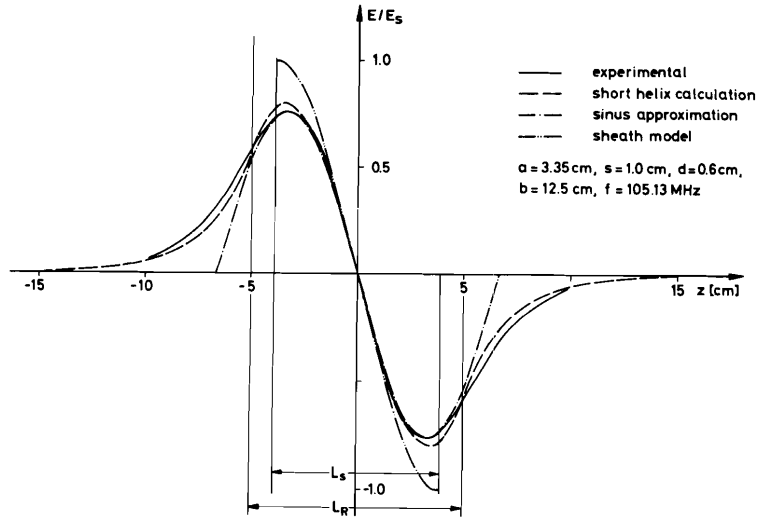

Fig. 4. Electrical fields on the axis for a $\lambda/2$ helix; power loss per unit length p = constant.

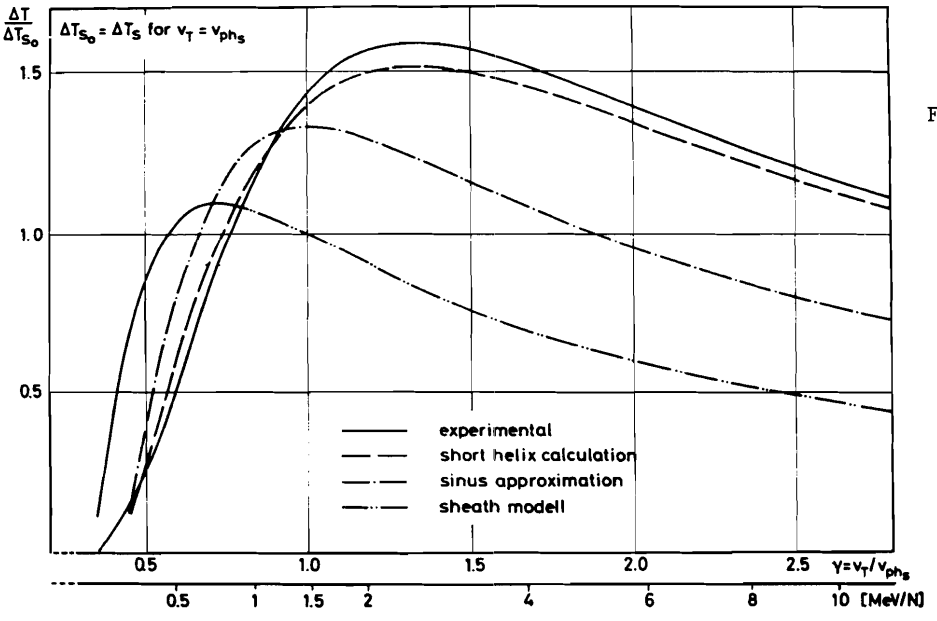

Fig. 5. Energy gain ΔT as a function of the particle velocity v_T compared with the energy gain ΔT_{s_o} in a sheath model-$\lambda/2$-helix with $v_T = v_{ph}$ (sheath) for the different fields given in Fig. 4.

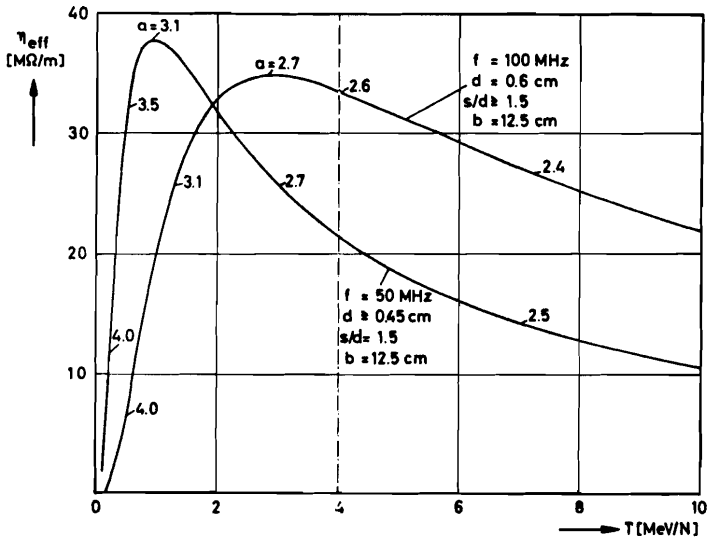

Fig. 6. Calculated maximum effective shuntimpedance η_{eff} as function of the particle energy T (p = const.):

$$\eta_{eff} = \frac{\Delta T_R^2}{\Delta T_{S_o}^2} \cdot \frac{L_s^2}{L_R^2} = \eta_{sheath} \cdot TT^2 .$$

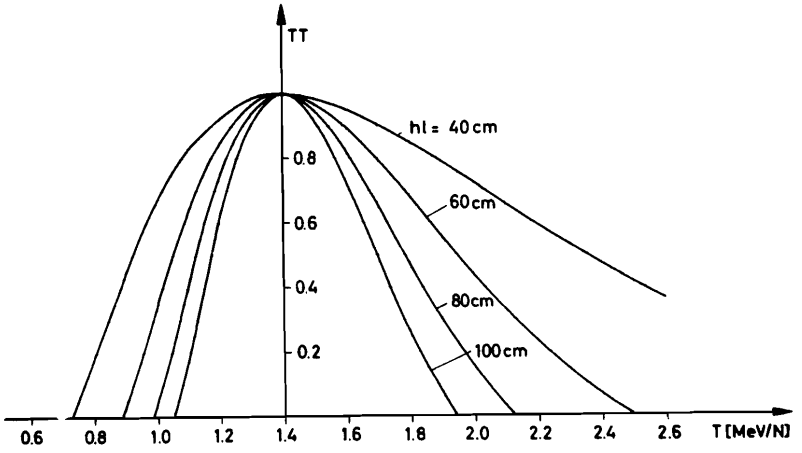

Fig. 7. Transit time factor at different helix section length. Energy 1.4 MeV/N.

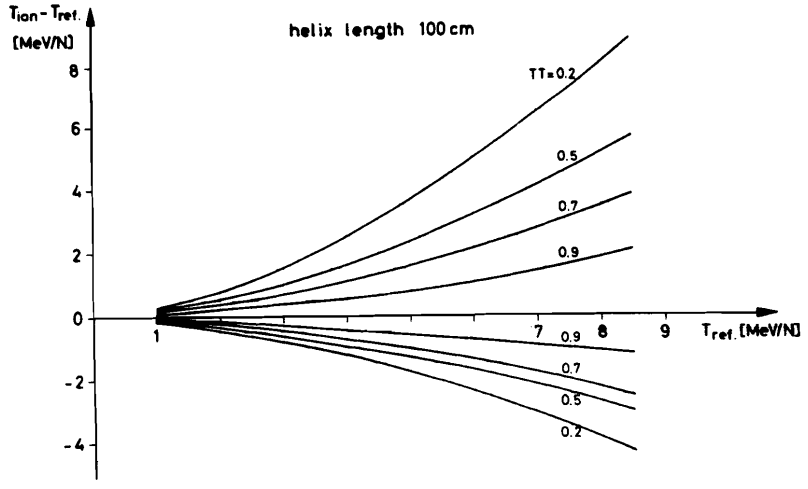

Fig. 8. Dependence of transit time factor on the energy ($v_{phase} = v_{particle}$).

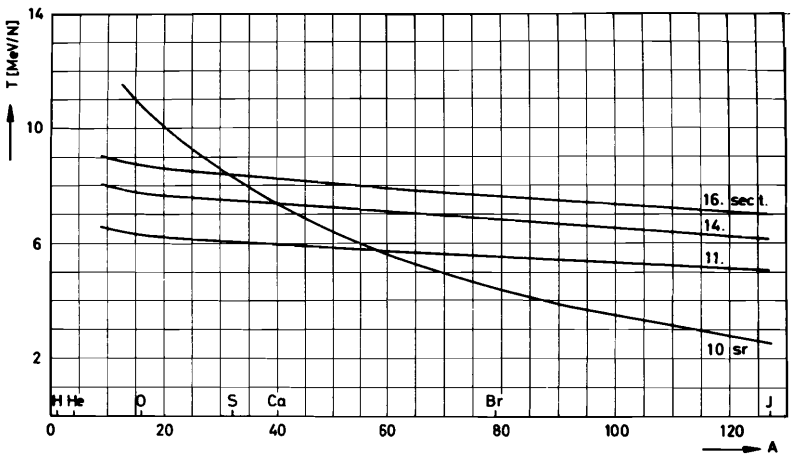

Fig. 9.
Maximum final energy as a function of the atomic mass number. Reference particle: $_{127}J^{30+}$ (q=0.236), T_{inj} =1.4MeV/N, Helix length 100cm, E_o = .8 MV/m.

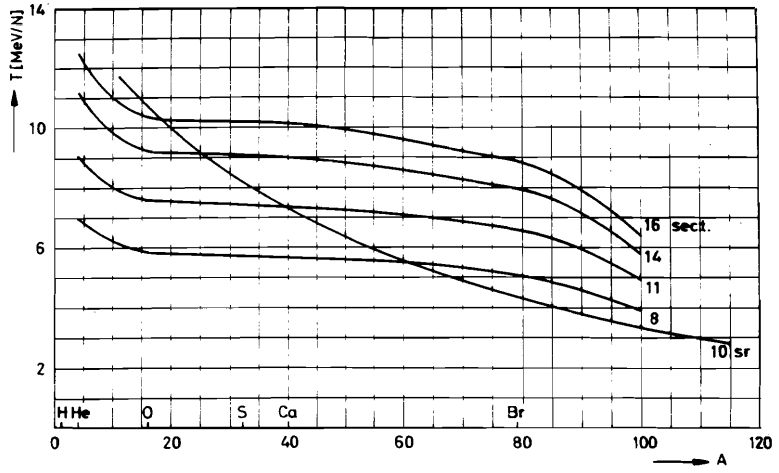

Fig. 10.
Maximum final energy as a function of the atomic mass number. Reference particle: $_{79}Br^{24+}$ (q =0.304), T_{inj} =1.36 MeV/N, Helix length 100cm, E_o =1.8 MV/m.

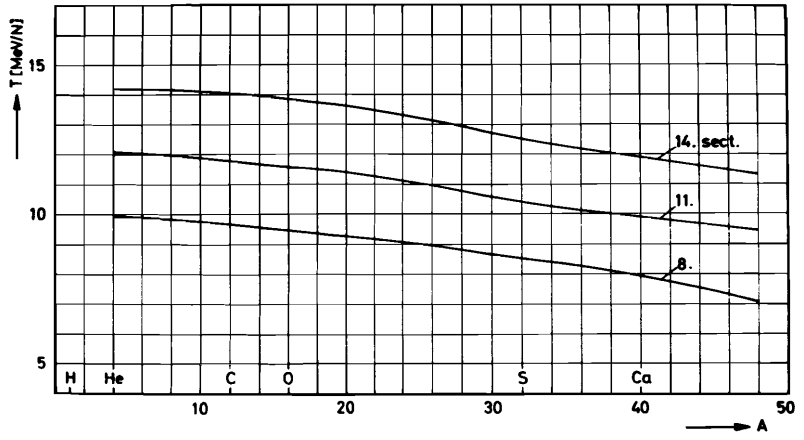

Fig. 11.
Maximum final energy as a function of the atomic mass number. Reference particle: $_{40}Ca^{17+}$ (q =0.425), T_{inj} = 2.7 MeV/N, Helix length 100cm, E_o =1.8 MV/m.

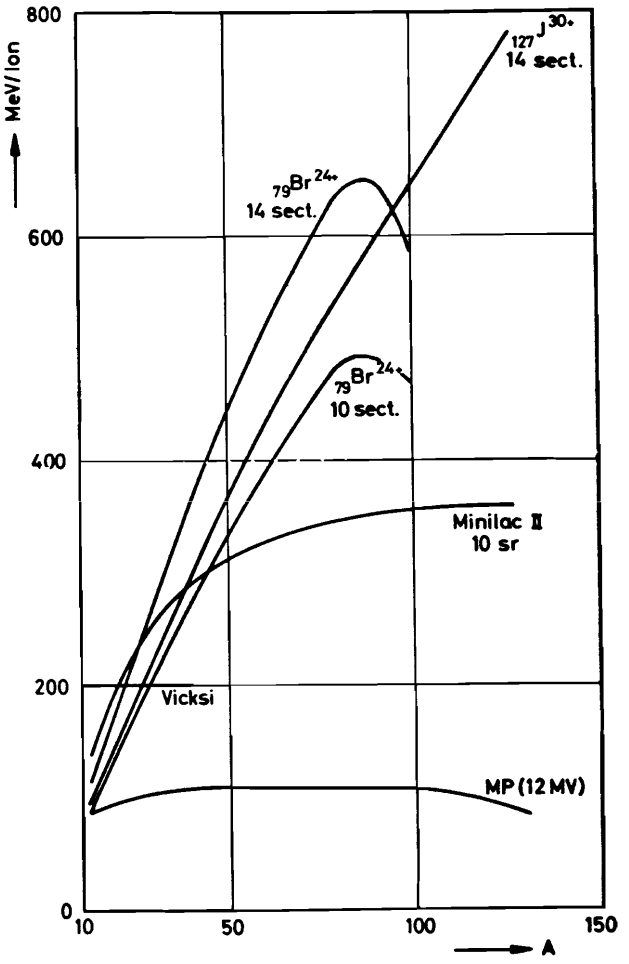

Fig. 12. Energy per ion for different accelerators.

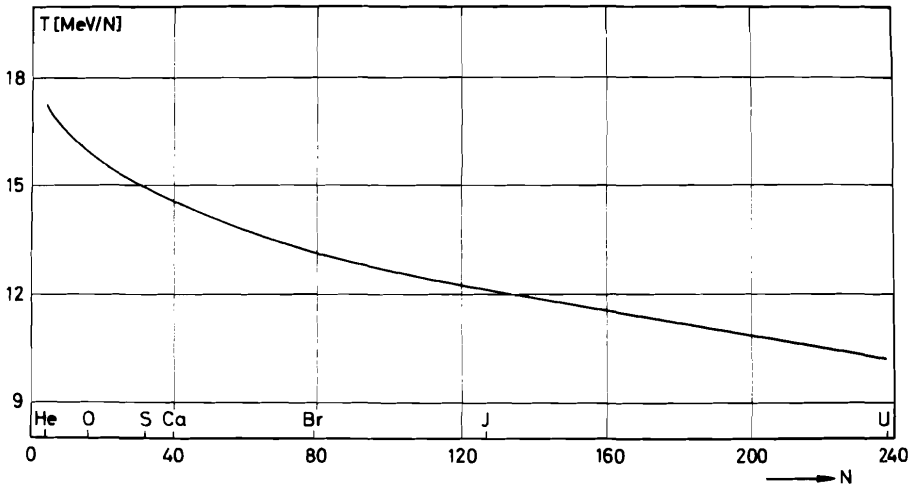

Fig. 13. Maximum energy versus atomic mass number. Foilstripper at 0.756 MeV/N.

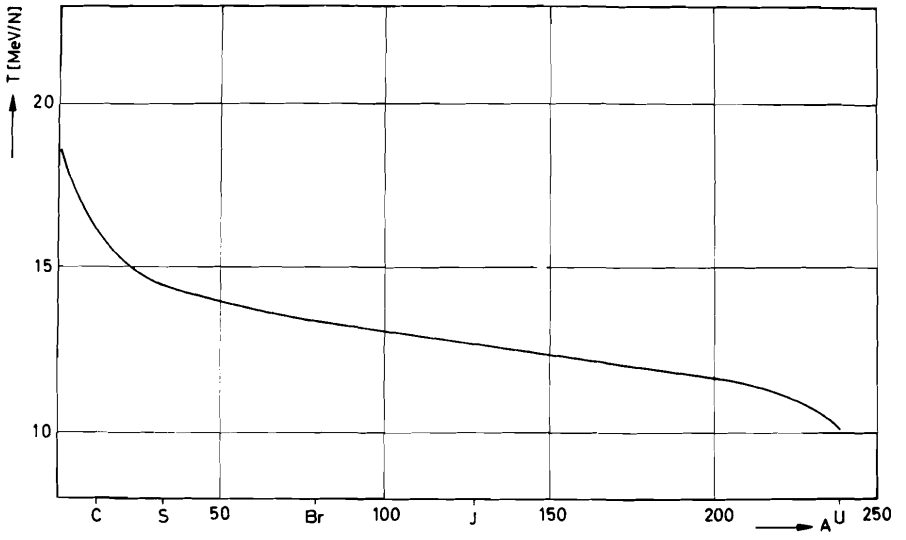

Fig. 14. Maximum energy versus atomic mass number; 30 sections, E_o = 2.3 MV/m; foilstripper at 1.1 MeV/N.

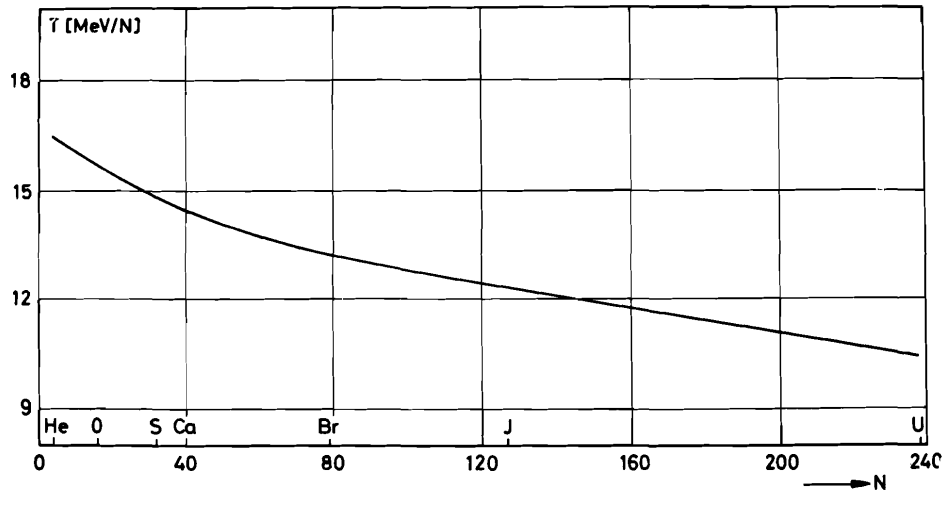

Fig. 15. Maximum energy versus atomic mass number. Foilstripper at 1.428 MeV/N.

Discussion

Miller, SLAC: How much does the shunt that stabilizes the helix drop the shunt impedance?

Klein: The shunt impedance doesn't drop. Calculations indicate that it should be within 1% and that's true, according to the measurement.

Miller: Does it effect the axial electric field profile?

Klein: No, it doesn't. Up to a detuning frequency of one megacycle or so.